Calculating Haze Parameter of Textured Transparent Conductive Oxides

A. Čampa* and M. Topič
University of Ljubljana, Faculty of Electrical Engineering
*Corresponding author: Tržaška 25, 1000 Ljubljana, Slovenia, andrej.campa@fe.uni-lj.si

Abstract: In thin-film solar cells (a-Si:H, µc-Si:H, CIGS, …) scattering of light is very important to increase absorption of light in the active layers of solar cells. Today the most efficient thin-film solar cells are designed or deposited on random textured transparent conductive oxides (TCO). In order to study the scattering properties of the surface texture we have developed a numerical model in COMSOL, which calculates the scattering parameters from atomic force microscopy scan of surface texture/topography. This way we can study and evaluate the texture capabilities to scatter the light before producing such a texture, thus reducing time and cost for studying new types of textured surfaces. The simulation results obtained from the numerical model were compared to measured values.

Keywords: Solar cells, surface textures, scattering parameters

1. Introduction

Optical characterization of complex structures and textures of interfaces between two layers presents one of the important issues in the design of thin-film solar cells. The rough surface texture between two materials scatters part of the light to oblique angles (in transmittance and reflectance), thus increasing the light path through layers. By prolonging the light path in active layers of thin-film solar cells the absorptance of light and efficiency of solar cell increases. By increasing the absorptance inside active layers, the overall thin-film thickness can be decreased, therefore the deposition times and costs related to deposition processes are reduced.

To study different surface textures or morphologies we have set up a numerical model to study the scattering capabilities of such a surface. The scattering is determined by the Haze parameter, Eq. 1. Haze parameter (H) determines the fraction of light that is scattered (diffused light (I_{dif})) at the interface compared to total intensity of light (I_{tot}, specular (I_{spec}) and diffused light).

$$H = \frac{I_{dif}}{I_{tot}} = \frac{I_{dif}}{I_{spec}+I_{dif}} \qquad (1)$$

The haze parameter is measured by means of Total Integrating Scattering measurements (TIS) [1]. The principle of measurement of haze in reflectance is shown in Fig 1.

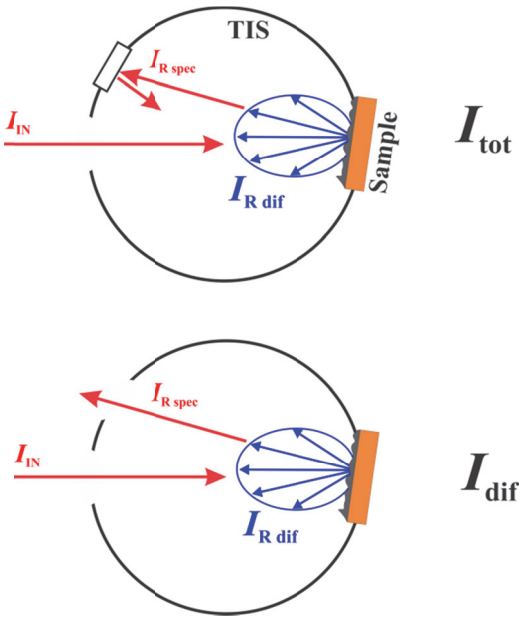

Figure 1. The principle of measuring I_{tot} and I_{dif} using a total integrating sphere.

The haze in reflectance is determined indirectly from measurements of total and diffused light. To gather the scattered light in the detector a total integrating sphere (also called Ulbricht sphere) is used. Putting on or off the spectralon reflector at the opening of the sphere, the specular beam signal can be captured or left out. This way the total and diffused reflectance can be measured, from which the haze can be calculated according to Eq. 1.

For our measurements we have used Perkin Elmer Lambda 950 spectrophotometer. The design and optimization of the surface texture is mainly regulated by the solar spectrum and the absorption coefficients of the layers. It is important to achieve a good scattering in the wavelength region of 500 nm to 1000 nm, where a part of the light is transmitted through the

absorptive layers. By prolonging the light path in the absorptive layer the quantum efficiency of solar cells increases and thus the solar cell efficiency improves. The haze parameter at a specific wavelength is calculated from the far-field domain. Two different approaches and models of obtaining the haze parameters are shown.

2. Numerical Model

The numerical models were prepared for a COMSOL simulation software version 4.2a with a Radio Frequency (RF) module. Two types of numerical models are presented, one model with an air-perfect electric conductor (PEC) interface and one model with a realistic interface between two custom materials.

2.1 Numerical model for air-PEC interface

The approach taken when building a numerical model is similar to the approach taken when measuring the haze parameter. The idea behind the model is to calculate the far-field intensity of the specular and diffused light separately. The easiest way to achieve this is by surrounding the studied surface by a sphere. Assuming the transmittance through the layer or reflectance from the subsequent interfaces is negligible, we can then surround the sample only by half of the sphere. Assuming the directions x and y in the sample are symmetrical, the model can be reduced to one eighth of the sphere, as shown in Fig. 2. The atomic force microscopy (AFM) scan of the textured TCO surface [2, 3] was imported to the numerical model. In Fig. 3 the AFM scan of widely used Asahi U type of TCO is presented [4]. The imported png image was constructed or approximated with a parametric surface, the maximum number of knots was set to 800. The imported surface was meshed with a triangular mesh, the maximum size was set to 20 nm, while the minimum size was set to 5 nm. The maximum size corresponds to the size of the point of the AFM scan. Reducing the size of the mesh would not produce better results from an optical point of view, while a larger size of the mesh may not take into account all the details of the morphology, therefore the increased size of the mesh may influence the scattering in the short wavelength region. For shorter wavelengths a more detailed mesh of the surface is required, since the small details in surface roughness already affect the scattering properties. However, the surface generation and transformation is slow, therefore we have generated only one surface with the same approximation for all wavelengths. It was generated for the worst case scenario (good approximation for the shortest wavelength).

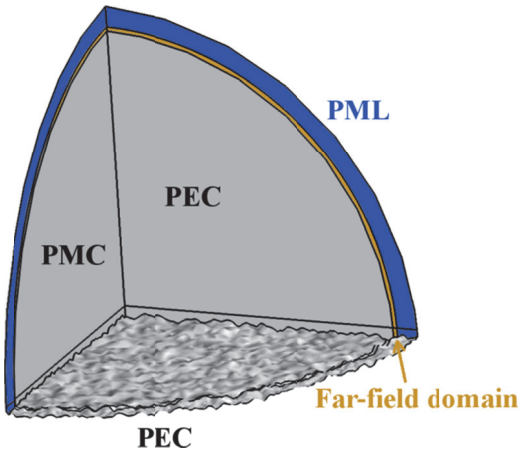

Figure 2. Numerical model for the air-PEC interface, showing the imported surface of TCO and boundary conditions at different edges of the model.

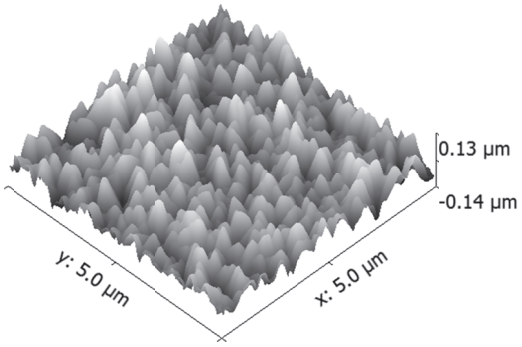

Figure 3. AFM scan of a textured TCO (Asahi U).

The numerical error can be decreased by setting more points of mesh resolution at the boundary condition and setting fewer points of mesh resolution at the inner boundary of the far-field domain. This way unwanted reflectance from the boundary condition can be reduced and the relatively slow post processing calculation of haze from the far-field can be sped up. By setting enough points at the textured surface and boundary condition, the rest of the domain can

be meshed with a lower number of points. The mesh size can be reduced even below the recommended minimum 10 points per wavelength to obtain good results.

At the edge, where the surface and the sphere intersect, we can expect a high, unwanted reflectivity from the PML, since a part of the incident field is reflected at the perpendicular angle back from the surface. Most of this light is then reflected back into the structure, the angle of incidence of backscattered light on the PML is close to 90 degrees. In order to reduce unwanted reflectance, we have generated a Gaussian beam instead of the plane wave. The Gaussian beam has a much lower intensity at the intersection of the studied surface and the sphere. The model was solved for scattered field and the Gaussian beam was generated for the background field according to Eq. 2.

$$E_b = e^{(i2\pi z/\lambda)} e^{-(x/w)^2} e^{-(y/w)^2} \hat{y} \qquad (2)$$

x, y and z are coordinates and w is the width of the Gaussian beam. In most cases the w was set to the same number as the radius of the domain.

2.2 Numerical model for the air-material interface

In most cases we are interested in how the light is scattered between two materials. We will show another model that takes into account two materials (in our case an air-realistic metal interface). Because we have a complex interface between two materials, we have decided to switch to a total field calculation, since the backscattered field cannot be simply defined. This time the incident Gaussian beam is defined at the scattering boundary condition and therefore the studied domain is not enclosed by the PML domain, Fig 4. At the bottom, bellow the studied material domain, the material was terminated by the scattering boundary condition. Other settings are the same, compared to the first model.

In Fig. 4 we can see how the far-field domain is divided into the specular and the diffused surface. The surface integration of far-field intensity (intensity is proportional to emw.normEfar^2) is performed on these surfaces to obtain the specular and the diffused intensity of light, from which the haze parameter is calculated. The width of the specular surface corresponds to the width of the incident aperture in the Lambda 950 spectrophotometer.

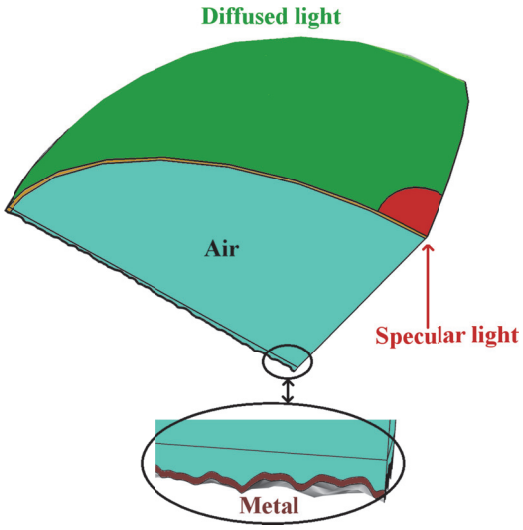

Figure 4. Numerical model for air-material interface, showing the specular and diffused far-field domain from which the haze parameter is calculated.

3. Results

Both models were tested on the same sample with the same isotropic morphology of the surface. The structures for verification consisted of the Asahi U TCO covered by a thin layer of aluminum. Thickness of the aluminum layer was around 100 nm. Aluminum has high reflectivity in the wide wavelength range (more than 90%), thus the air-PEC model might be utilized. The measured wavelength dependent complex refractive index of aluminum was imported to COMSOL in order to obtain good results. The haze parameter was calculated in the range between 500 and 1000 nm with the step size of 50 nm, measurements were done every 10 nm. However, the haze parameter does not change rapidly, thus fewer steps were taken in the simulations.

In Fig. 5 the results of the simulation for air-PEC (symbols) and the air-material (black curve) model are shown and compared to the measured values (red curve). Good agreement is obtained between the measurements and the simulations for both numerical models. The wavelength dependent complex refractive index ($N(\lambda) = n(\lambda) - ik(\lambda)$) values for aluminum, used in the model, are summarized in Table 1.

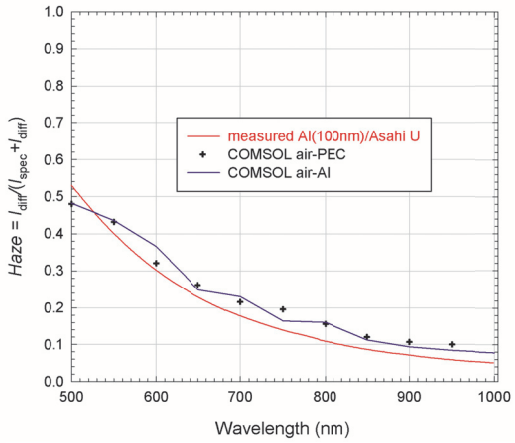

Figure 5. Simulated haze in reflection for the air-PEC interface (symbols) and for the air-Al interface (black curve) and measured haze for the air-Al textured interface (red curve).

Table 1: Wavelength dependent refractive index of thin-film aluminum used in the simulations

Al/wavelength λ [nm]	$n(\lambda)$	$k(\lambda)$
1000	1.34	10.72
950	1.51	8.90
900	2.08	8.36
850	2.54	8.2
800	2.68	8.46
750	2.36	8.58
700	1.85	8.3
650	1.47	7.78
600	1.20	7.26
550	0.95	6.68
500	0.76	6.07

Since the air-material model uses an ordinary scattering boundary condition and the not more advanced PML boundary condition as the air-PEC model, we conducted a set of simulations with different widths of the studied domain. In Fig. 6 results for 3 different domain widths are shown: 5000 nm, 6000 nm and 7500 nm, the width of Gaussian beam was set to 5000 nm in all three cases. If we increase the domain size we get better results, especially in the long wavelength region. However, in all simulations, we observe the same trend with a higher deviation in the long wavelength region. In order to obtain good results in the long wavelength region, the Gaussian beam has to be greater than a few wavelengths. The dispersion of the beam is directly related to the ratio between the wavelength and the Gaussian beam width. In order to eliminate the dispersion due to the Gaussian beam, its width should be more than 5 wavelengths [5].

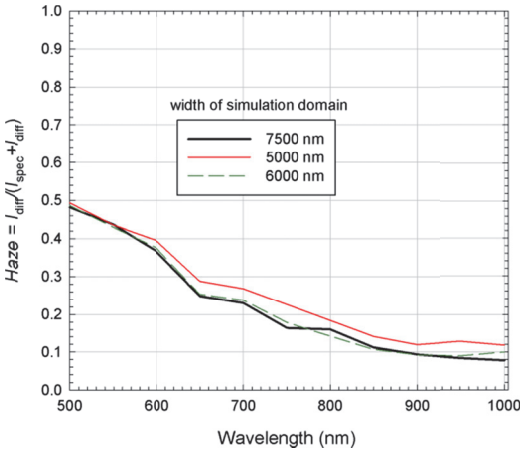

Figure 6. Comparison of simulation results for different widths of the domain (reference 7500 nm) with the same width of the Gaussian beam (5000 nm).

In Fig. 7 two cases are shown with different widths of the Gaussian beam (5000 nm and 7500 nm). In both cases we see bending of the electric field (encircled), which is the consequence of a less than ideal boundary condition. The bending is more pronounced for a wider Gaussian beam. The boundary condition does not work well for high incident angles, the part of light is reflected back into the domain. At the intersection of the domain with a studied surface the boundary condition acts as a waveguide for high incident angles, which is then translated into bending of the electric field. The error can be suppressed by a bigger domain or a narrower Gaussian beam. In most cases the width of the Gaussian beam can be set to the width of the domain to obtain eligible results.

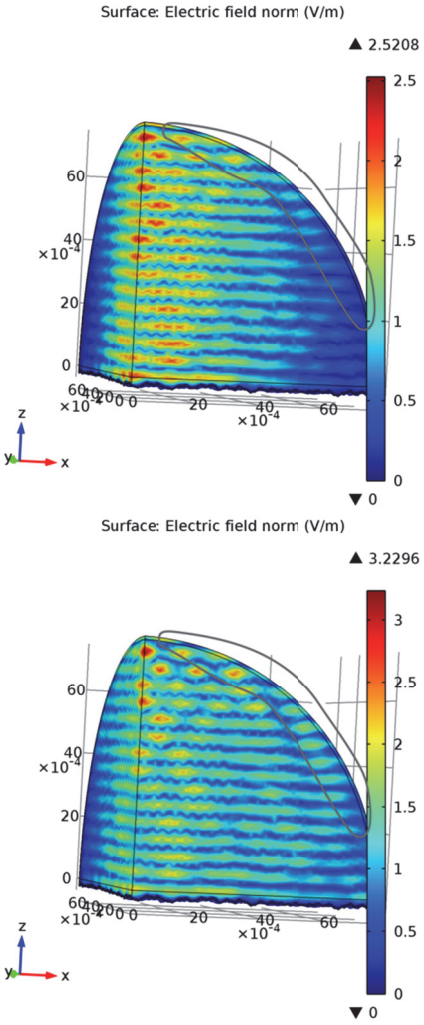

Figure 7. Bending of electric field due to less than ideal boundary condition. In the second example (width of Gaussian beam is 7500 nm) the bending is more pronounced than in the first case (width of the Gaussian beam is 5000 nm).

3.1 Anisotropic surface

In the case of an anisotropic surface (directional dependent surface texture) the same model can be used. However, we have to make two sets of simulations to take into account both polarizations (TE wave and TM wave). We conducted the simulation of the surface as described by Heijna [6]. In this case the grating surface was reproduced with an ideal sine and rectangular gratings width a period of 1000 nm and an amplitude of 300 nm. The results are shown in Fig. 8. The tendency of the simulated haze is the same compared to the measured haze as presented in Fig. 6a in [6]. In Fig. 8 the Haze for TE (green dashed curve) and TM wave (red dashed curve) are also shown, along with the haze for unpolarized light (black solid curve) for sine shaped gratings. The peak in the Haze at 800 nm is related to the first diffraction order of grating, while the peak at 400 nm is related to the second diffraction order according to the grating equation [7]. For comparison, the simulated unpolarized haze for a rectangular shape is presented (blue solid line). The main deviation between the measured and the simulated haze is that we have used an approximated grating shape (rectangular and sine), however the tendency in the haze was as expected for both approximations, compared to measured U-shaped gratings. The described grating structure could be solved with 2D simulations, however our purpose was to show the correctness of the model used for anisotropic structures.

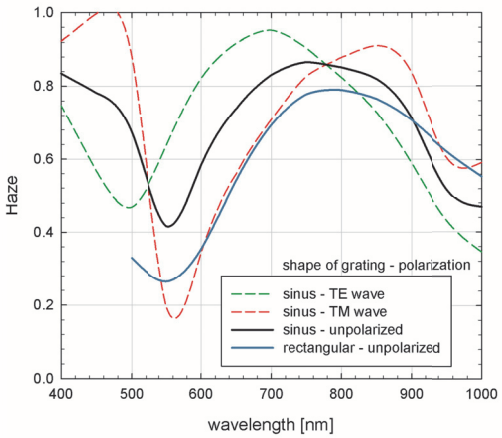

Figure 8. The calculated haze functions in reflection for sinus diffraction grating (black solid curve) for the TE and TM wave (dashed curves) and for rectangular grating (blue solid curve).

7. Conclusions

The scattering of light from the textured surfaces is very important in thin-film solar cells. We have demonstrated that the relatively simple numerical model can be used for determination of scattering parameter haze provided the AFM scans of textured surface are available. Two different models were shown and their differences were discussed. The possible errors from numerical modeling were suppressed in

order to obtain credible numerical results. The model was verified on a realistic isotropic TCO structure and on an anisotropic grating structure.

8. References

1. J.M. Bennett, L. Mattsson, *Introduction to Surface Roughneess and Scattering*, Optical Society of America, Washington D.C. (1989)
2. S. Faÿ, J. Steinhauser, N. Oliveira, E. Vallat-Sauvain, C. Ballif, Opto-electronic properties of rough LP-CVD ZnO:B for use as TCO in thin-film silicon solar cells, *Thin Solid Films*, 515, p. 8558-8561 (2007)
3. J. Müller, B. Recha, J. Springer, Milan Vanecek, TCO and light trapping in silicon thin film solar cells, *Solar Energy*, 77, p. 917 (2004)
4. Sato, K., Y. Gotoh, Y. Hayashi, K. Adachi, H. Naishimura, Highly Textured SnO_2 TCO Films for a-Si Solar Cells, *Reports of the Research Laboratory*, Asahi Glass Co., Ltd. 40, p. 129 (1992)
5. A. Čampa, *Modelling and optimization of advanced optical concepts in thin-film solar cells*, PhD Thesis, Ljubljana (2010)
6. M.C.R. Heijna, J. Löffler, B.B. Van Aken, W.J. Soppe, H. Borg, P.G.J.M. Peeters, Nanoimprint lithography of light trapping patterns in sol-gel coatings for thin film silicon solar cells, *Proceedings of SPIE* 7002, Strasbourg (2008)
7. C. Heine, R.H. Morf, Submicrometer gratings for solar energy applications, *Applied Optics*, 34, p. 2476 (1995)